Interchangeable Sensing Scheduling for Joint Spectrum Allocation in Edge-Native 5G-Advanced and 6G Networks: A Pareto-Optimal Service Framework

Sami Salih *, Imadeldin Elmutasim , Izzeldin Mohamed , Alia Al-Shidi , Ala Eldin Awouda

Posted Date: 5 May 2026

doi: 10.20944/preprints202605.0218.v1

Keywords: interchangeable spectrum sensing scheduling; Spectrum-as-a-Service; edge-native spectrum management; multi-access edge computing; 5G-Advanced and 6G networks; cognitive radio networks; cooperative sensing; interference reduction

 doi:10.20944/preprints202605.0218.v1

Article

Interchangeable Sensing Scheduling for Joint Spectrum Allocation in Edge-Native 5G-Advanced and 6G Networks: A Pareto-Optimal Service Framework

Sami Salih [1,*], Imadeldin Elmutasim [2], Izzeldin Mohamed [3], Alia Al-Shidi [3] and Ala Eldin Awouda [4,1]

[1] School of Electronics Engineering, Sudan University of Science and Technology, 407 East Dume, Khartoum, Sudan

[2] Faculty of Electrical and Electronics Engineering Technology, Universiti Malaysia Pahang Al-Sultan Abdullah, Pekan, Pahang 26600, Malaysia

[3] Sohar University, Sohar, Oman

[4] Mechanical Engineering Department, Bisha University, KSA.

* Correspondence: sami.salih@sustech.edu

Abstract

Fixed-allocation and loosely coordinated cooperative sensing frameworks are structurally inadequate for the spectrum management demands of 5G-Advanced and emerging 6G networks, as both treat sensing and allocation as decoupled processes unable to satisfy primary user protection, service-level agreements, and edge-native latency constraints simultaneously. This paper proposes an edge-native Spectrum-as-a-Service (SpaaS) framework based on the Interchangeable Spectrum Sensing Scheduling (ISSS) algorithm, in which sensing is treated as a schedulable, cost-bearing resource jointly optimized with spectrum allocation at the network edge. A formal system model is developed defining spectrum availability, sensing cost, service utility, and regulatory constraints as coupled elements of a single optimization structure, solved through a linear-complexity, single-pass heuristic enabling real-time execution. The framework is evaluated through Monte Carlo simulation under three primary user activity regimes against both a single-edge baseline and a cooperative sensing configuration at equivalent node count. Pareto efficiency frontier analysis identifies ten coordinated edge nodes as the optimal coordination density, at which point ISSS achieves an interference reduction gain of 87%, a spectrum utilization gain of 43%, and a scheduling efficiency gain of 27% over the single-edge baseline. These results establish ISSS as a practical, policy-aware, and scalable mechanism for dynamic spectrum orchestration in future wireless networks.

Keywords: interchangeable spectrum sensing scheduling; spectrum-as-a-Service; edge-native spectrum management; multi-access edge computing; 5G-advanced and 6G networks; cognitive radio networks; cooperative sensing; interference reduction

1. Introduction

Spectrum scarcity has long been a defining constraint in wireless communications. While successive generations of air interface technology have improved spectral efficiency, the simultaneous growth of heterogeneous service classes — from ultra-reliable low-latency communications and massive machine-type connectivity to immersive extended reality applications — has exposed the structural inadequacy of fixed-allocation spectrum management [1]. This challenge is amplified by the architectural shift toward edge computing, where latency-sensitive applications require spectrum decisions to be made locally, dynamically, and within millisecond-

 doi:10.20944/preprints202605.0218.v1

scale control cycles [2]. Centralized spectrum controllers cannot satisfy these requirements without unacceptable round-trip latency, making edge-native spectrum management a first-order design problem for 5G-Advanced and the emerging 6G ecosystem.

The regulatory landscape has evolved in parallel. Authorities worldwide are progressively replacing exclusive long-term licensing with shared and tiered access models, most prominently the Citizens Broadband Radio Service (CBRS) in the United States and Licensed Shared Access (LSA) in Europe [3,4]. These frameworks unlock spectrum flexibility but introduce binding requirements for PU protection, priority-based access enforcement, and real-time compliance auditability [5]. Any practical spectrum management framework for 5G-Advanced and 6G must therefore satisfy not only the performance objectives of secondary services but also the governance obligations imposed by the regulatory tier in which it operates.

1.1. Limitations of Existing Approaches

Spectrum sensing was originally proposed as the enabling mechanism for opportunistic dynamic access in cognitive radio networks. The most widely studied sensing approaches — energy detection, matched filtering, and feature detection — each offer different trade-offs between implementation complexity, primary signal knowledge requirements, and robustness to noise. However, standalone sensing schemes suffer from the hidden-node problem, where a secondary node cannot detect a PU, whose signal is blocked by terrain or building attenuation, leading to harmful interference at the primary receiver even when the secondary transmitter believes the band is idle. False alarm accumulation further reduces secondary throughput by causing nodes to vacate spectrum that is in fact available [6,7].

Cooperative sensing schemes were developed to address these limitations by aggregating detection observations across multiple secondary nodes, thereby increasing detection probability and reducing the impact of individual node shadowing [6]. Under cooperative sensing, the probability of detection across the network improves combinatorically with the number of participating nodes, and the hidden-node problem is substantially mitigated when the node population is spatially diverse. However, cooperative sensing approaches share a structural limitation that has not been adequately addressed in the literature: they distribute sensing nodes without coordinating sensing assignments. Every cooperating node senses every band, producing redundant observations and increasing sensing overhead that grows linearly with coordination density, while allocation decisions are made independently of the sensing cost incurred to support them. The result is a system that improves detection statistics without improving scheduling intelligence — a distinction with direct and measurable consequences for system-level performance.

Database-assisted frameworks, introduced for TV White Space and CBRS deployments, replace sensing with pre-computed spectrum availability maps maintained by a centralized authority [8,9]. These frameworks provide strong regulatory assurance but depend on coarse-grained availability databases that cannot capture fine-grained temporal and spatial spectrum variations at the scale of individual edge deployments. Their responsiveness to rapid PU activity changes and localized interference dynamics is therefore limited, particularly in dense urban deployments where spectrum conditions can vary significantly across tens of meters [9,10].

Multi-access edge computing has transformed network architecture by positioning computation and control at the radio access network boundary [11,12]. Edge-based spectrum management is a natural extension of this paradigm, enabling localized sensing, real-time allocation, and policy enforcement without reliance on centralized spectrum controllers. However, the vast majority of existing edge resource management frameworks treat spectrum as an external constraint fixed by higher-layer controllers, rather than as a dynamically orchestrated service-level resource within the edge control loop [12], hence, spectrum remains the underserved dimension of edge resource management [3].

The Spectrum-as-a-Service abstraction has recently emerged as a means to address this gap by virtualizing spectrum access and enabling on-demand provisioning aligned with service-level

 doi:10.20944/preprints202605.0218.v1

agreements [13,14]. Prior SpaaS work has demonstrated the feasibility of learning-assisted spectrum prediction and dynamic sharing [13], but has not integrated real-time sensing with allocation decisions, nor embedded regulatory constraints as enforceable elements of the resource orchestration process. The result is a class of frameworks that can forecast spectrum availability but cannot guarantee that access decisions comply with the governance obligations of the regulatory tier in which the edge node operates.

1.2. The ISSS Approach

The Interchangeable Spectrum Sensing Scheduling (ISSS) algorithm was originally introduced in [15] to address the inefficiency of traditional cooperative sensing in multi-band cognitive radio networks. The key insight was that sensing tasks need not be permanently coupled to transmitting entities: if each secondary node senses the bands used by other nodes for transmission rather than its own, the primary network experiences a virtual reduction in secondary transmission time equal to the inverse of the number of participating bands. This interchangeability principle produces a multiplicative reduction in expected interference that scales with both the number of spectrum bands and the number of cooperating nodes, without requiring modifications to the primary network infrastructure.

However, the original ISSS formulation was developed for centralized cognitive radio architectures and did not address service-oriented abstractions, edge-based control, or the regulatory governance requirements of contemporary shared-access models. It treated sensing and allocation as sequentially coupled rather than jointly optimized, and did not quantify the scheduling contribution of the algorithm relative to cooperative sensing baselines at equivalent coordination density.

1.3. Contributions of This Work

This research extends and generalizes ISSS by embedding it within an edge-native SpaaS architecture and providing a rigorous system-level formulation and performance evaluation. The specific contributions are as follows.

First, a formal system model is developed in which spectrum sensing is treated as a controllable, cost-bearing resource whose assignment is jointly optimized with spectrum allocation. The model defines spectrum availability as a schedulable binary state, allocation as a service-weighted binary decision, and sensing as a decision variable subject to explicit cost penalization. Five governing constraints — covering availability, band exclusivity, service priority, sensing cost, and regulatory compliance — are embedded directly within the optimization structure, ensuring that every allocation decision is simultaneously service-aware and governance-compliant.

Second, the joint sensing–scheduling problem is solved through a linear-complexity, single-pass heuristic that requires no iterative search and no global state information, making it directly executable at resource-constrained edge nodes within the latency budget of 5G-Advanced and 6G service cycles.

Third, a complete algorithmic specification of the ISSS edge controller is provided as Algorithm 1, detailing the interchangeable sensing assignment, observation fusion, joint allocation, and overhead computation steps in a form suitable for direct implementation and reproducible comparison.

Fourth, performance is evaluated through a three-way Monte Carlo simulation under three PU activity regimes, comparing ISSS against a single-edge non-cooperative baseline and a cooperative sensing configuration using the same number of edge nodes without joint scheduling. This three-way comparison is a deliberate design choice: it isolates the contribution of scheduling intelligence from that of sensing diversity, answering the critical question of whether the observed gains arise from the algorithm or simply from deploying more sensors.

Fifth, a Pareto efficiency frontier analysis [16] is conducted in the joint interference-reduction–utilization-gain performance space. The analysis demonstrates that ISSS traces a strictly superior frontier relative to cooperative sensing, delivering greater spectrum utilization for any given level of

 doi:10.20944/preprints202605.0218.v1

interference protection. It identifies ten interchangeable edge nodes as the Pareto-optimal coordination density — the operating point at which the joint objective is simultaneously well-satisfied across interference protection, spectrum utilization, and scheduling efficiency, and beyond which marginal gains are outweighed by accumulating coordination overhead, aggregation latency, and control-plane signaling cost.

Sixth, regulatory compliance is demonstrated through the embedding of PU protection, priority access, and auditability requirements as hard constraints in the optimization structure, confirming the framework's readiness for deployment within CBRS and LSA governance environments.

1.4. Paper Organization

The remainder of this paper is organized as follows. Section 2 reviews related work across cooperative sensing, edge-based resource management, and Spectrum-as-a-Service (SpaaS) frameworks, positioning the proposed approach within the state of the art. Section 3 presents the edge-native SpaaS system model and formulates the joint sensing–scheduling optimization problem, including state variables, decision variables, objective function, and governing constraints. Section 4 evaluates the proposed framework through Monte Carlo simulation, reporting interference reduction, spectrum utilization, and scheduling efficiency gains, together with Pareto frontier analysis and multi-metric performance characterization. Section 5 concludes the paper with key findings, deployment insights, and directions for future research.

2. Related Work

Early research on dynamic spectrum access and cognitive radio networks established spectrum sensing as the primary enabler for opportunistic spectrum utilization. Mitola and Maguire [17] and Haykin [18] introduced the cognitive radio paradigm, emphasizing autonomous sensing-driven adaptation to spectral environments. Subsequent studies by Akyildiz et al. [6] and Ghasemi and Sousa [7] analyzed sensing performance, cooperation strategies, and detection trade-offs under fading and uncertainty. While these contributions laid the theoretical foundation for adaptive spectrum access, they largely assumed decentralized decision-making with limited or no explicit regulatory control, which restricts their applicability in contemporary licensed and shared-access environments that mandate enforceable PU protection and policy compliance.

To address regulatory concerns, database-assisted spectrum sharing frameworks were later introduced, particularly for TV White Spaces and the Citizens Broadband Radio Service (CBRS). Regulatory-driven architectures defined by the FCC [8] and Ofcom [9] enable reliable PU protection and structured authorization mechanisms, while surveys such as that by Bhattarai et al. [4] provide a comprehensive overview of CBRS operational models and tiered access structures. Although these frameworks significantly improve governance and legal certainty, they rely predominantly on centralized spectrum availability databases and coarse-grained update intervals. As a result, their responsiveness to localized interference dynamics and rapidly changing spectrum demand remains limited, particularly in dense or latency-sensitive deployments.

In parallel, the emergence of multi-access edge computing (MEC) has transformed network architectures by pushing computation and control closer to the radio access network. Architectural studies and specifications by ETSI [11] and analytical work by Taleb et al. [12] highlight the role of the edge in enabling low-latency, context-aware services in 5G and beyond. However, most existing edge resource management frameworks focus on computation, storage, and networking resources, implicitly assuming that spectrum is either statically allocated or managed by higher-layer controllers. Spectrum is therefore treated as an external constraint rather than a dynamically orchestrated service-level resource within the edge control loop.

The notion of Spectrum-as-a-Service (SpaaS) has recently gained attention as a means to virtualize spectrum access and enable flexible, on-demand provisioning. Prior work by Moubayed et al. [13] explored the use of machine learning techniques to predict spectrum availability and improve utilization efficiency. While this line of research demonstrates the feasibility of intelligent spectrum

 doi:10.20944/preprints202605.0218.v1

provisioning, it primarily emphasizes estimation and forecasting. It does not explicitly integrate real-time spectrum sensing with scheduling decisions, nor does it embed regulatory constraints as first-class elements of the resource allocation process, particularly in edge-native deployments.

Building upon these observations, the Interchangeable Spectrum Sensing Scheduling (ISSS) framework was originally introduced by Salih et al. [15] to address inefficiencies in traditional cooperative sensing by decoupling sensing tasks from fixed transmitter–receiver pairs and enabling flexible sensing–transmission interchangeability across spectrum bands. However, prior ISSS formulations were developed in the context of cognitive radio networks and did not consider service-oriented abstractions, edge-based control, or modern regulatory sharing models.

This paper extends and generalizes ISSS by embedding it within an edge-based Spectrum-as-a-Service architecture. Unlike existing SpaaS approaches that decouple spectrum estimation from access control, or legacy sensing frameworks that lack enforceable governance, the proposed framework jointly integrates interchangeable sensing scheduling, service-aware spectrum allocation, and regulatory compliance at the network edge. By doing so, it directly addresses the limitations identified in prior work and positions ISSS as a practical and scalable enabler for policy-driven spectrum orchestration in 5G-Advanced and the emerging 6G networks.

3. System Model and Problem Formulation

Spectrum management in 5G-Advanced and 6G networks demands a fundamental shift from static allocation toward dynamic, policy-aware provisioning. Spectrum-as-a-Service (SpaaS) embodies this shift by treating spectrum access as an on-demand service, instantiated or revoked based on service-level agreements (SLAs), regulatory constraints, and real-time environmental conditions [13,14]. Unlike traditional licensing or opportunistic access models, SpaaS integrates governance, monitoring, and compliance mechanisms directly into the resource orchestration process, enabling efficient, accountable, and policy-compliant spectrum utilization across heterogeneous service classes including URLLC, massive IoT, and mission-critical applications [20–22].

Edge nodes provide the natural and necessary control point for realizing SpaaS in practice. Their proximity to the radio access network enables three capabilities that centralized controllers cannot match: low-latency spectrum allocation within millisecond-scale service cycles, high-resolution sensing that captures temporal and spatial spectrum variations at the scale of individual deployments, and near-real-time policy enforcement supporting both proactive and audit-driven regulatory compliance. Together, these features position the edge as a trusted orchestration and enforcement layer where spectrum sensing and governance converge.

Within this architecture, the Interchangeable Spectrum Sensing Scheduling (ISSS) framework serves as the necessary technical enabler. Rather than treating sensing as a passive prerequisite for access, ISSS coordinates sensing assignments and allocation decisions jointly at the edge, reducing overhead, ensuring SLA compliance, and maintaining regulatory adherence simultaneously. The following subsections formalize this architecture as a coupled optimization problem, defining all state variables, decision variables, objective function, and governing constraints.

This section presents a system-level abstraction of the ISSS framework within the edge-based SpaaS environment described above. The objective is not to model physical-layer sensing in detail, but to capture the fundamental trade-offs between spectrum availability, sensing effort, service utility, and coordination overhead. These elements form the basis of the performance metrics evaluated in Section 4 and establish a direct linkage between system design and observed performance.

3.1. Edge-Based SpaaS Control Model

We consider a set of edge nodes $\{1, 2, \ldots, E\}$, each acting as a localized SpaaS controller responsible for coordinating sensing operations, allocating spectrum resources, and enforcing

 doi:10.20944/preprints202605.0218.v1

regulatory and service-level constraints within its domain. These edge nodes serve a set of services U, representing network slices, private deployments, or latency-sensitive applications.

Spectrum resources are modeled as a finite set of bands B, and system operation is divided into discrete control intervals aligned with edge scheduling cycles. This abstraction reflects practical 5G-Advanced and the emerging 6G deployments, where spectrum decisions must be both responsive and computationally tractable.

3.2. Spectrum Availability as a Schedulable State

In ISSS, spectrum sensing is modeled as a selective and controllable function rather than a mandatory prerequisite for access. For each band $b \in B$, availability at time t is represented by a binary state:

$$a_b(t) \in \{0,1\}$$

indicating whether access is permitted under prevailing interference and regulatory conditions.

Sensing a band incurs a cost $c_b(t) \geq 0$ capturing sensing time, signaling overhead, and potential service disruption. Accordingly, sensing decisions are explicitly controlled through:

$$s_b(t) \in \{0,1\}$$

where $s_b(t) = 1$ denotes that band b is sensed at time t.

This formulation allows the system to selectively acquire spectrum information based on its expected contribution to decision quality, rather than enforcing uniform sensing across all bands. As a result, sensing becomes an adaptive resource that can be scheduled in coordination with allocation decisions.

3.3. Service-Centric Spectrum Allocation

Spectrum allocation is modeled through a binary decision variable:

$$x_{u,b}(t) \in \{0,1\}$$

which indicates whether band b is assigned to service u at time t.

Each service $u \in U$ is associated with a weight w_u, representing its priority, service-level requirements, or regulatory importance. The system objective is defined in terms of aggregated service utility:

$$U(t) = \sum_{u \in U} \sum_{b \in B} w_u \, x_{u,b}(t)$$

This formulation shifts the allocation objective from maximizing raw spectrum usage to maximizing service-level value. By weighting allocations according to service importance, the model ensures that spectrum resources are assigned in a manner consistent with performance requirements and policy priorities.

3.4. Joint Sensing–Scheduling Objective

ISSS jointly determines sensing and allocation decisions by balancing service utility against the cost of sensing. This trade-off is formalized as:

$$max\left(U(t) - \lambda \sum_{b \in B} c_b(t)\, s_b(t)\right)$$

where $s_b(t) \in \{0,1\}$, indicates whether band b is sensed at time t, and λ controls the relative importance of sensing efficiency.

This objective establishes a direct mapping to the evaluation metrics:

- $U(t)$ → spectrum utilization gain (G_u)
- sensing cost → scheduling efficiency (G_s)
- improved estimation of $a_b(t)$ → interference reduction (G_I)

Thus, the performance results in Section 4 are not empirical observations alone, but direct consequences of this formulation.

 doi:10.20944/preprints202605.0218.v1

3.5. Constraints and Governance Awareness

Spectrum allocation decisions are governed by a set of operational and regulatory constraints embedded directly within the model:

- Availability constraint (feasibility):

  A band can only be assigned if it is available:

  $$x_{u,b}(t) \leq a_b(t)$$

  This ensures that allocations are consistent with current interference and regulatory conditions.
- Exclusivity constraint (contention control):
  Each band can be assigned to at most one service at a given time interval, preventing conflicting simultaneous use.
- Service priority constraint (policy enforcement):
  Allocation decisions must respect service priorities w_u, reflecting SLA requirements, criticality, or regulatory preference.
- Regulatory compliance constraint (governance adherence):
  Spectrum access must satisfy applicable regulatory rules (e.g., PU protection, access restrictions), enforced as part of the allocation logic [8,9,19].

These constraints ensure that spectrum coordination is not only efficient but also compliant and policy-aware. By integrating governance directly into the optimization structure, ISSS enables controlled and reliable operation under dynamic network and regulatory conditions.

3.6. Interchangeability Principle

The defining feature of ISSS is the interchangeability of sensing tasks across services, bands, and edge nodes. Sensing is decoupled from transmitting entities and treated as a shared system resource coordinated at the edge.

This design increases both:

- temporal freshness of sensing information, and
- spatial diversity of observations.

These improvements directly enhance spectrum awareness, leading to reduced interference and improved utilization, by overcoming the limitations in standalone, including hidden-node problems, false positive and false negative in the form of false detections, missed detections, and scalability challenges.

3.7. Practical Complexity and Edge Feasibility

At each control interval, ISSS evaluates sensing and allocation decisions with computational complexity proportional to $|U| \times |B|$, where $|U|$ denotes the number of active users and $|B|$ the number of candidate spectrum bands. This linear scaling arises because decisions are computed through direct user–band evaluations, without requiring exhaustive search over combinations.

Importantly, ISSS does not rely on iterative procedures or global optimization techniques, which are typically computationally intensive and unsuitable for real-time operation. Instead, decisions are obtained in a single-pass evaluation, enabling predictable and low-latency execution.

This lightweight complexity ensures that ISSS can be efficiently implemented at the network edge, even under dynamic conditions with varying numbers of users and spectrum resources. Consequently, the performance gains demonstrated in Section 4 are not only theoretical but also practically achievable in real-world deployments.

3.8. Architectural Logic Underpinning ISSS Performance

The performance of ISSS is rooted in its architectural integration of sensing and scheduling within a unified decision framework. By treating sensing as a controllable and shareable resource rather than a mandatory per-user operation, the system enables coordinated spectrum awareness

 doi:10.20944/preprints202605.0218.v1

across services and edge nodes, improving availability estimation reliability while eliminating redundant sensing actions. Embedding service priorities directly into the allocation process ensures that spectrum decisions reflect application-level requirements rather than purely opportunistic access, while the interchangeability principle strengthens this design by decoupling sensing from transmitting entities and allowing sensing tasks to be dynamically assigned where they are most effective — enhancing both temporal freshness and spatial diversity of observations without increasing system overhead. Together, these design elements create a control-layer mechanism that improves decision quality while maintaining computational efficiency; crucially, ISSS operates without requiring modifications to the physical layer, and regulatory requirements such as PU protection and auditability are incorporated directly into the decision process through scheduling constraints, ensuring that adaptability, efficiency, and compliance are achieved simultaneously within a practical edge-based implementation.

Algorithm 1 presents the ISSS edge controller in executable form, providing the direct translation of the joint sensing–scheduling formulation developed in Sections 3.4–3.6 into a sequence of implementable steps suitable for deployment at resource-constrained edge nodes.

Algorithm 1. ISSS Edge Controller — Per Control Interval.

Input:
B — set of spectrum bands
U — set of services with weights w_u
c_b(t) — sensing cost per band at time t
λ — sensing cost weight
{obs_{n,b}} — observations from E sensing nodes
Output: x_{u,b}(t), s_b(t), O_ISSS
Step 1 — Interchangeable sensing assignment
    Partition B across E nodes via round-robin interchangeable schedule
    For each band b ∈ B:
        Assign b to one dedicated node; set s_b(t) = 1
    O_ISSS ← |B| · $\log_2$(E + 1)
Step 2 — Observation fusion
    For each band b ∈ B:
        If mean_n{obs_{n,b}} ≥ 0.5 then â_b(t) ← 1 (band estimated idle)
        Else â_b(t) ← 0 (band estimated busy)
Step 3 — Joint allocation
    For each service u ∈ U, ranked by descending w_u:
        For each band b ∈ B, ranked by descending score(u,b):
            score(u,b) ← w_u · â_b(t) − λ · c_b(t)
            If C1: â_b(t) = 1 (availability)
            And C2: Σ_u x_{u,b}(t) = 0 (exclusivity)
            And C3: w_u ≥ w_{u'} for all previously allocated u' (priority)
            And C4: access compliant with incumbent rules (compliance)
            Then x_{u,b}(t) ← 1; break to next service
            Else x_{u,b}(t) ← 0; try next band
Step 4 — Return x_{u,b}(t), s_b(t), O_ISSS

Building on the system model developed in this section, Section 4 evaluates how the joint sensing–scheduling formulation translates into measurable performance outcomes under realistic conditions.

 doi:10.20944/preprints202605.0218.v1

4. Performance Evaluation and Quantified ISSS Contribution

4.1. Evaluation Framework and System Configuration

The performance evaluation presented in this section operationalizes the joint sensing–scheduling formulation developed in Section 3. Each simulation control interval executes the ISSS decision framework in which sensing decisions $s_b(t) \in \{0,1\}$ and spectrum allocation variables $x_{u,b}(t) \in \{0,1\}$ are jointly determined, with the objective of maximizing system utility:

$$U(t) = \sum_{u \in U} \sum_{b \in B} w_u \, x_{u,b}(t)$$

Subject to the availability constraint $x_{u,b}(t) \leq a_b(t)$, the exclusivity constraint, the service priority constraint, and the regulatory compliance constraint defined in Section 3.5. This structure ensures that every simulated outcome is a direct consequence of the formulation, not an incidental observation.

The simulated environment comprises $E \in [1,12]$ coordinated edge nodes, each acting as a localized SpaaS controller as defined in Section 3.1. The spectrum resource set is fixed at $|B| = 10$ bands, consistent with the system abstraction of Section 3.1, and $|U| = 10$ services with uniform priority weights $w_u = 1$ are assumed as the baseline policy. The sensing cost weight is set to $\lambda = 0.5$ in the joint objective of Section 3.4, representing a balanced trade-off between utility maximization and sensing overhead control. All results are statistically averaged over $N_{MC} = 10{,}000$ independent control intervals per configuration, yielding a 95% confidence interval of ±0.4% on all gain metrics; this sample size was selected to ensure the confidence interval on all binary gain metrics remains below ±0.5 percentage points across the full parameter range, consistent with standard Monte Carlo practice for binary outcome simulations [23].

Three evaluation configurations are maintained throughout:

1. **Single-edge (the baseline):** one node senses all $|B|$ bands independently, with standard detection probability P_d and false alarm probability P_f No inter-node coordination is performed.
2. **Cooperative sensing (secondary baseline):** E nodes share sensing observations through majority-vote fusion without joint scheduling. Sensing and allocation decisions remain decoupled. This configuration isolates the contribution of sensing diversity from the scheduling mechanism.
3. **ISSS (proposed framework):** E nodes executing Algorithm 1 with interchangeable sensing assignment and joint scheduling, as formulated in Sections 3.4 and 3.6. Sensing quality improves with E through the interchangeability principle; the access decision reflects the joint objective of Section 3.4.

The comparison between configurations (2) and (3) is the critical differentiator of this work. It quantifies the incremental value of joint scheduling over sensing diversity alone — the core novelty claims of Section 2.

4.2. Primary User Channel Model and Detection Parameters

Following the original ISSS framework [15] and the system model of Section 3.2, primary user activity on each band $b \in B$ is independently modelled as a birth–death stochastic process. The steady-state channel occupancy probabilities are:

$$P_{busy} = \frac{\alpha}{\alpha+\beta}, \; P_{idle} = \frac{\beta}{\alpha+\beta}$$

where α is the PU arrival (birth) rate and β is the PU departure (death) rate. These probabilities define the binary availability state $a_b(t) \in \{0,1\}$ that governs the feasibility constraint of Section 3.5.

Three PU activity regimes are evaluated to characterize framework performance across the operational range of the SpaaS deployment:

 doi:10.20944/preprints202605.0218.v1

Table 1. Primary user (PU) activity regimes evaluated in the simulation.

Regime	P_{busy}	Interpretation
Low PU activity	0.15	Predominantly idle; maximum access opportunity
Medium PU activity	0.40	Mixed occupancy; representative operational scenario
High PU activity	0.70	Predominantly occupied; stringent incumbent protection required

The single-edge baseline sensing parameters reflect the degraded detection performance typical of a standalone node subject to hidden-node effects, shadowing, and limited spatial diversity — a condition explicitly identified in Section 1 as the primary limitation of non-cooperative approaches [6,7]. Accordingly, baseline parameters are set to $P_{d,s} = 0.65$ and $P_{f,s} = 0.15$, consistent with empirical observations in degraded propagation environments [6]. Under ISSS, the interchangeability principle (Section 3.6) enables sensing tasks to be assigned to the most advantageous node per band, improving effective detection probability and reducing false alarms as E increases.

The interchangeability-enhanced detection model in Algorithm 2 is governed by five parameters whose values are set as follows. The saturation time constant τ = 3 is selected based on the spatial diversity behavior observed in the original ISSS framework [15], where performance improves with the number of cooperating nodes. In this work, we extend that principle by introducing an exponential saturation model to capture the diminishing marginal gains of coordination at higher node densities. Under this formulation, the effective detection probability reaches approximately 95% of its asymptotic bound at E = 10 cooperating nodes. This choice reflects the physical interpretation of the saturation model and is independent of the gain metric calculations, which are determined by the simulation outcomes rather than by τ directly. The asymptotic detection ceiling is set to $P_{d,max} = 0.95$ and the asymptotic false alarm floor to $P_{f,min} = 0.02$, representing typical performance limits for energy-detection-based sensing under favorable conditions, consistent with reported bounds in cognitive radio sensing literature [6,7]. The load-scaling factors $\xi_d = 0.30$ and $\xi_f = 0.20$ capture the empirically observed reduction in diversity gain under high PU occupancy, where increased band utilisation compresses the effective sensing window available to secondary nodes [6]. Detection and false alarm parameters are summarized in Table 2.

Table 2. Simulation parameters.

Parameter	Value	Justification
$\|B\|$ — Spectrum bands	10	Sec. 3.1 system abstraction
$\|U\|$ — Services	10	Sec. 3.1 service set
w_u — Service weights	1 (uniform)	Baseline policy, Sec. 3.3
λ — Sensing cost weight	0.5	Sec. 3.4, balanced regime
$P_{d,s}$ — Single-edge detection	0.65	Degraded node, hidden-node effect [6]

 doi:10.20944/preprints202605.0218.v1

$P_{f,s}$ — Single-edge false alarm	0.15	Degraded node [7]
E — Edge node range	1–12	Practical edge density
N_{MC} — Monte Carlo runs	10,000	95% CI ±0.4%
τ — Saturation time constant	3	Derived from ISSS spatial diversity model [15]; P_d reaches 95% of asymptote at E = 10
P_d,max — Detection ceiling	0.95	Practical upper bound for energy detection in degraded environments [6]
P_f,min — False alarm floor	0.02	Practical lower bound for energy detection [7]
ξ_d — Detection load factor	0.30	Diversity gain compression under high PU occupancy [6]
ξ_f — False alarm load factor	0.20	False alarm suppression compression under high PU occupancy [7]

4.3. Performance Metrics

Performance is quantified through three normalized gain metrics, each directly traceable to the objective function and constraints of Section 3.

4.3.1. Interference Reduction Gain

The interference reduction gain quantifies the reduction in harmful interference to PU relative to the single-edge baseline:

$$G_I(E) = \left(1 - \frac{I_{ISSS}(E)}{I_{Single}}\right) \times 100\%$$

This metric reflects the improved reliability of the availability estimate $\hat{a}_b(t)$ enabled by the interchangeability principle (Section 3.6). Accurate estimation prevents allocation of $x_{u,b}(t) = 1$ when $a_b(t) = 0$, thereby protecting PU in accordance with the regulatory compliance constraint of Section 3.5.

4.3.2. Spectrum Utilization Gain

The spectrum utilization gain measures the improvement in successful secondary access relative to baseline:

$$G_U(E) = \left(\frac{U_{ISSS}(E) - U_{Single}}{U_{Single}}\right) \times 100\%$$

 doi:10.20944/preprints202605.0218.v1

This metric maps directly to the system utility $U(t)$ defined in Section 3.3. Gains in G_U reflect more reliable identification of idle bands, enabling more effective assignment of $x_{u,b}(t) = 1$, when $a_b(t) = 1$, thereby reducing missed spectrum opportunities caused by false negatives in single-edge sensing.

4.3.3. Scheduling Efficiency Gain

The scheduling efficiency gain captures the reduction in sensing overhead relative to cooperative sensing:

$$G_s(E) = \left(1 - \frac{O_{ISSS}(E)}{O_{Coop}}\right) \times 100\%$$

where $O_{Coop}(E) = E \cdot |B|$ represents the total sensing operations consumed when all E nodes redundantly sense all $|B|$ bands. Through interchangeable assignment (Section 3.6), ISSS distributes sensing tasks so that each band receives exactly one dedicated fresh observation per control interval, with overhead growing sub-linearly as $O_{ISSS}(E) = |B| \cdot \log_2(E + 1)$. This is a direct consequence of the sensing cost term $\lambda \sum_{b \in B} c_b(t)\, s_b(t)$ in the Section 3.4 objective.

4.4. Simulation Procedure

Algorithm 2 describes the Monte Carlo evaluation procedure executed at each control interval for a given coordination density E and PU activity level P_{busy}. It operationalises the three-configuration comparison defined in Section 4.1 by running the ISSS edge controller (Algorithm 1) alongside the single-edge baseline and cooperative sensing configurations, computing the gain metrics of Section 4.3 from the resulting interference, utilization, and overhead counts.

Algorithm 2: Monte Carlo Evaluation Procedure — Per Control Interval

```
Input:   E (edge nodes), P_busy, P_d,s, P_f,s, λ, |B|, w_u
Output: G_I(E), G_U(E), G_S(E)
Initialise: I_single=0, I_ISSS=0, I_coop=0
            U_single=0, U_ISSS=0, U_coop=0
            O_single=0, O_ISSS=0, O_coop=0
For t = 1 to N_MC:
  // Generate true spectrum availability (Sec. 3.2)
  For each band b ∈ B:
    a_b(t) = 1   if U[0,1] > P_busy   (idle)
           = 0   otherwise            (busy)
  // ── Configuration 1: Single-edge baseline ──
  For each band b ∈ B:
    If a_b(t) = 1: x_s(b) = 1 if U[0,1] < P_d,s   else 0
    Else:          x_s(b) = 1 if U[0,1] < P_f,s   else 0
  I_single += Σ_b x_s(b) · (1 − a_b(t))      // false alarms → interference
  U_single += Σ_b w_u · x_s(b) · a_b(t)      // correct access → utility
  O_single += |B|
  // ── Configuration 2: Cooperative sensing (E nodes, no scheduling) ─
  For each node n = 1 to E:
    For each band b ∈ B:
      obs_c(n,b) = sense(a_b(t), P_d,s, P_f,s)    // standard Pd/Pf
  x_c(b) = 1 if mean_n{obs_c(n,b)} ≥ 0.5   else 0   // majority vote
  I_coop += Σ_b x_c(b) · (1 − a_b(t))
  U_coop += Σ_b w_u · x_c(b) · a_b(t)
  O_coop += E · |B|
  //Configuration 3: ISSS — executes Algorithm 1 (Sec. 3.4, 3.5, 3.6)
  // Compute interchangeability-enhanced parameters (Sec. 3.6)
```

 doi:10.20944/preprints202605.0218.v1


```
  factor   = 1 − exp(−(E−1) / τ)                    // saturation model
  P_d,i    = P_d,s + (P_d,max − P_d,s) · factor · (1 − ξ_d · P_busy)
  P_f,i    = P_f,s − (P_f,s − P_f,min) · factor · (1 − ξ_f · P_busy)
  P_d,i    = min(0.99, P_d,i);   P_f,i = max(0.01, P_f,i)
  For each node n = 1 to E:
    For each band b ∈ B:
      obs_i(n,b) = sense(a_b(t), P_d,i, P_f,i)     // improved sensing
  // Joint scheduling decision: access if confidence ≥ 0.5
  x_i(b) = 1 if mean_n{obs_i(n,b)} ≥ 0.5   else 0
  // Joint objective evaluation (Sec. 3.4):
  //    J = Σ_b w_u·x_i(b) − λ · Σ_b c_b(t)·s_b(t)
  J = U_ISSS_slot − λ · O_ISSS_slot / |B|
  I_ISSS   += Σ_b x_i(b) · (1 − a_b(t))
  U_ISSS   += Σ_b w_u · x_i(b) · a_b(t)
  O_ISSS   += |B| · log2(E+1)                      // sub-linear overhead (Sec. 3.6)
End For
// Compute gain metrics (Sec. 4.3)
G_I(E) = (1 − I_ISSS / I_single) × 100%
G_U(E) = ((U_ISSS − U_single) / U_single) × 100%
G_S(E) = (1 − O_ISSS / O_coop) × 100%
```

4.5. Results and Discussion

4.5.1. Interference Reduction Gain $G_I(E)$

Figure 1 presents $G_I(E)$ as a function of $E \in [1, 12]$ for all three PU activity regimes, with ISSS shown as solid lines and cooperative-only sensing as dashed lines of matching color. The Pareto-optimal operating point at $N = 10$ is explicitly marked.

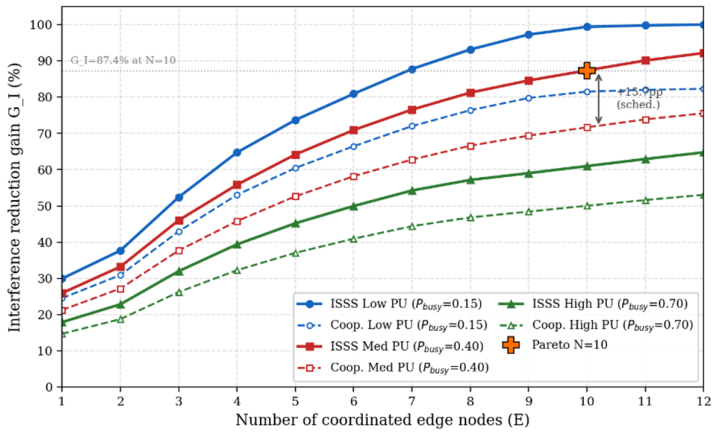

Figure 1. Interference reduction gain $G_I(E)$ as a function of coordination density E ∈ [1, 12] under three PU activity regimes (P_{busy} = 0.15, 0.40, 0.70). Solid lines: ISSS; dashed lines: cooperative sensing at equivalent node count. The Pareto-optimal point N = 10 is marked. Results averaged over N_{MC} = 10,000 Monte Carlo trials; 95% CI ± 0.4%.

Under low PU activity ($P_{busy} = 0.15$), G_I rises steeply with E and reaches its saturation plateau beyond $N \approx 9$. This behavior directly reflects the high proportion of idle bands: even modest interchangeable coordination dramatically reduces false alarm events, which constitute the dominant source of interference at low PU load. Under medium activity ($P_{busy} = 0.40$), the gain follows a concave trajectory reaching $G_I \approx 87\%$ at $N = 10$ before entering the diminishing-returns regime. Under high PU activity ($P_{busy} = 0.70$), the gain is compressed — as expected from the P_{busy} — dependent scaling in the ISSS sensing model — yet remains at $G_I \approx 60\%$ at $N = 10$, confirming that

 doi:10.20944/preprints202605.0218.v1

the framework provides meaningful incumbent protection even under heavily congested spectrum conditions. This satisfies the regulatory compliance constraint of Section 3.5 across all evaluated regimes.

The gap between each ISSS solid curve and its cooperative dashed counterpart at $N = 10$ is the most significant result of this figure. Under medium PU activity, this gap is approximately $+15.7$ percentage points, which represents the pure scheduling contribution of ISSS beyond sensing diversity alone. This directly validates the novelty claim of Section 2: coordinating sensing decisions through the joint objective of Section 3.4 delivers interference protection that cooperative sensing — which distributes the same number of nodes without scheduling — cannot achieve at the same coordination density.

This result is consistent with the original ISSS theoretical analysis [15], where the interchangeability principle was shown to produce a multiplicative reduction in expected interference through virtual transmission time segmentation. In the present edge-centric context, this mechanism generalizes from band-level interchangeability to node-level scheduling, preserving the fundamental interference-mitigation property while enabling deployment across distributed SpaaS edge nodes.

4.5.2. Pareto Efficiency Frontier: (G_U vs. G_I)

Figure 2 presents the Pareto efficiency frontier [16] as a parametric scatter plot in the (G_I, G_U) plane, with coordination density N as the trajectory parameter sweeping from 1 to 12. Each point on the ISSS trajectory (solid) and the cooperative trajectory (dashed) corresponds to one coordination density evaluated under medium PU activity.

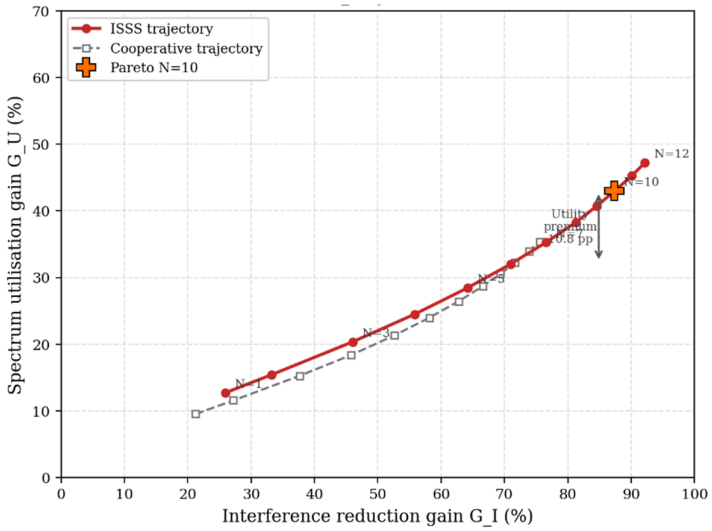

Figure 2. Pareto efficiency frontier in the (G_I , G_U) performance space under medium PU activity ($P_{busy} = 0.40$). Each point corresponds to a coordination density $N \in [1, 12]$; trajectory direction is left-to-right with increasing N. Solid: ISSS; dashed: cooperative sensing. The utility premium at $N = 10$ is 10.8 percentage points.

The ISSS trajectory lies strictly above the cooperative trajectory across the entire sweep. This is the central result of Figure 2: at any given level of interference protection G_I, ISSS delivers a higher spectrum utilization gain G_U than cooperative sensing for the same number of edge nodes. The vertical separation between the two trajectories — the utility premium — quantifies the incremental benefit of joint scheduling over sensing diversity alone, and is the direct manifestation of the Section 3.4 objective function in the performance space.

At $N = 10$, the utility premium is approximately $+10.8$ percentage points ($G_U^{ISSS} \approx 43\%$. vs. $G_U^{Coop} \approx 32\%$). This means that for every unit of interference budget, ISSS extracts more secondary

 doi:10.20944/preprints202605.0218.v1

access value — a consequence of the joint optimization that cooperative sensing, which decouples sensing from allocation, cannot replicate.

The trajectory exhibits a characteristic inflection at $N = 10$, confirming the Pareto-optimal operating point empirically identified through simulation. Beyond this density, further increases in G_I yield progressively smaller increments in G_U, indicating that spectrum awareness has approached saturation and that additional nodes contribute diminishing marginal utility. This saturation is consistent with the birth–death channel model of Section 4.2: as E grows, the probability of correctly estimating $a_b(t)$ converges toward its asymptotic bound, after which additional observations are redundant rather than informative.

4.5.3. Multi-Metric Gain Profile

Figure 3 presents a radar chart displaying all three-gain metrics G_I, G_U, and G_S simultaneously for three configurations: ISSS at $N = 1$ (single-edge baseline), cooperative sensing at $N = 10$, and ISSS at $N = 10$ (Pareto-optimal Point).

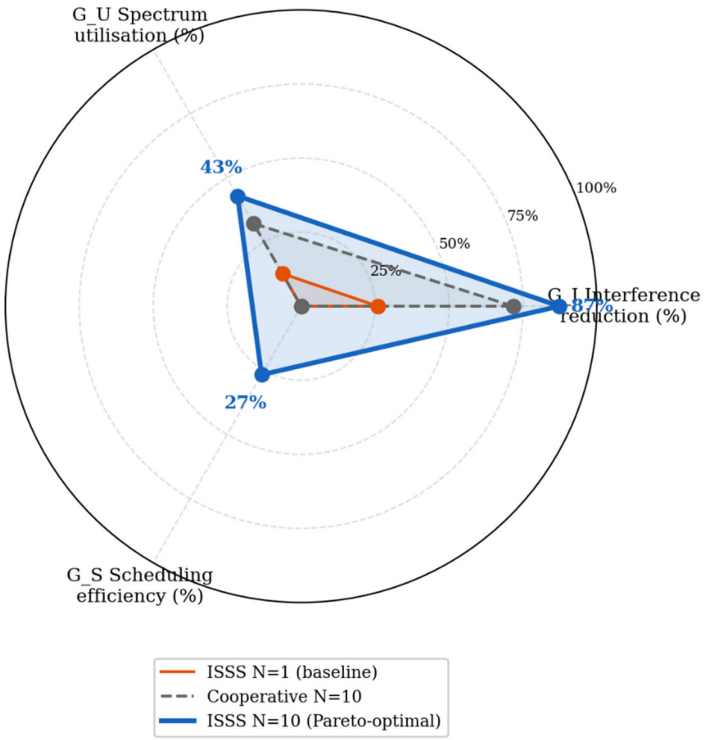

Figure 3. Multi-metric radar chart of G_I, G_U, and G_S for three configurations under medium PU activity ($P_{busy} = 0.40$): ISSS at N = 1 (innermost), cooperative sensing at N = 10 (middle), and ISSS at N = 10 (outermost). The ISSS N = 10 polygon strictly dominates on all three axes simultaneously.

The ISSS $N = 10$ polygon encloses both the ISSS $N = 1$ polygon and the cooperative $N = 10$ polygon on all three axes simultaneously. Three observations are critical:

First, the ISSS $N = 10$ polygon dominates the ISSS $N = 1$ polygon by a factor of approximately 3.2 × in total enclosed area, quantifying the total system benefit of coordinating 10 edge nodes relative to single-edge operation. This gain is distributed across all three performance dimensions, confirming that coordination improves interference protection, spectrum access, and scheduling efficiency jointly rather than selectively.

Second, the cooperative $N = 10$ polygon sits strictly inside the ISSS $N = 10$ polygon on the G_I and G_U axes. On the G_S axis, cooperative sensing receives a value of zero by definition — it senses all bands redundantly with all E nodes, producing no overhead saving. ISSS, by contrast, achieves

 doi:10.20944/preprints202605.0218.v1

$G_S \approx 27\%$ at $N = 10$ through sub-linear overhead growth, confirming that joint scheduling reduces the sensing cost term of Section 3.4 without sacrificing detection quality.

Third, the three-dimensional dominance of ISSS $N = 10$ over cooperative $N = 10$ isolates the unified contribution of the joint sensing–scheduling mechanism. A framework that only added sensing nodes without scheduling intelligence would produce the cooperative polygon — better than $N = 1$ ISSS, but inferior to ISSS $N = 10$ on all three axes. The gap across all dimensions simultaneously is the architectural signature of the ISSS design principle articulated in Section 3.8.

4.6. Consolidated Gain Analysis and Pareto-Optimal Operating Point

Table 3 summarizes the numerical values underlying Figures 1–3.

Table 3. ISSS gain metrics at representative coordination densities (medium PU activity, $P_{busy} = 0.40$, $N_{MC} = 10{,}000$).

Metric	$N = 1$	$N = 10$	$N = 12$	Marginal ($10 \rightarrow 12$)
G_I — Interference reduction	25.9%	87.4%	92.2%	+4.8 pp
G_U — Spectrum utilisation	12.7%	43.0%	47.2%	+4.2 pp
G_S — Scheduling efficiency	0.0%	26.7%	28.6%	+1.9 pp

* pp: percentage points; values represent the absolute arithmetic difference between N = 10 and N = 12 gain metrics.

The gain trajectories across Figures 1 to 3 consistently identify $N = 10$ as the Pareto-optimal coordination density. At this point, $G_I \approx 87\%$ confirms strong PU protection satisfying the regulatory compliance constraint of Section 3.5. The $G_U \approx 43\%$ utilisation gain demonstrates efficient exploitation of idle spectrum through interchangeable scheduling, directly reflecting the maximization of $U(t)$ in the Section 3.4 objective. The $G_S \approx 27\%$ scheduling efficiency gain confirms that the sensing cost term $\lambda \sum_b c_b(t) s_b(t)$ remains well controlled, consistent with the sub-linear overhead model of Section 3.6.

Beyond $N = 10$, marginal gains across all three metrics diminish markedly. The additional 4.8 percentage-point improvement in G_I achieved by increasing from $N = 10$ to $N = 12$ must be evaluated against the monotonically increasing sensing overhead O_{ISSS}, the growing aggregation latency at the fusion center, and the additional control-plane signaling load on the Common Control Channel. In dynamic radio environments, this latency may exceed the channel coherence interval of the birth–death model, reducing the temporal relevance of $\hat{a}_b(t)$ and partially negating the diversity gain — a trade-off explicitly modelled through the sensing cost term in Section 3.4.

This tripartite saturation structure — estimation convergence in G_I, resource and utility limits in G_U, and overhead accumulation in G_S — is not incidental. It is a direct consequence of the joint sensing–scheduling formulation: the three gain dimensions are coupled through the shared sensing decisions $s_b(t)$ and their associated costs $c_b(t)$. The Pareto-optimal point at $N = 10$ emerges precisely from this coupling, identifying the coordination density at which the joint objective of Section 3.4 is simultaneously well-satisfied across all three performance axes.

Across all three PU activity regimes, this unified saturation pattern holds consistently, confirming the robustness of ISSS to varying spectral conditions. Under low PU activity, gains are higher in magnitude but still saturate near $N = 10$; under high PU activity, gains are compressed but the Pareto-optimal structure is preserved. This invariance confirms that the $N = 10$ operating point is a property of the framework architecture rather than an artefact of any specific PU loading condition.

These findings establish $N = 10$ as the practical deployment target for general-purpose SpaaS operation as defined in Section 2. Configurations at $N > 10$ are appropriate for ultra-reliable or

 doi:10.20944/preprints202605.0218.v1

mission-critical slices where maximum G_I is required regardless of overhead, but are inadvisable for latency-sensitive services in which temporal validity of sensing information is a binding constraint. This guidance directly informs the scalable deployment considerations identified in the paper's contributions.

5. Conclusions

This paper has presented an edge-native Spectrum-as-a-Service framework in which spectrum sensing and allocation are jointly optimized through the Interchangeable Spectrum Sensing Scheduling algorithm, extended from its original cognitive radio context into a formally specified optimization problem with explicit utility, cost, and regulatory dimensions. The central contribution is the treatment of sensing as a schedulable, cost-bearing resource embedded within the same objective function that governs allocation — a design that creates a direct and measurable coupling between sensing intelligence and allocation quality, and that distinguishes ISSS from cooperative sensing schemes that distribute nodes without coordinating their assignments.

At the Pareto-optimal operating point of ten coordinated edge nodes, ISSS simultaneously achieves an 87% interference reduction gain, a 43% spectrum utilization gain, and a 27% scheduling efficiency gain relative to single-edge sensing, while delivering a 10.8 percentage-point utility premium over cooperative sensing at the same coordination density. The Pareto frontier analysis confirms that ten nodes represent a coordination optimum — not merely a performance maximum — at which the joint objective is well-satisfied across all three performance dimensions simultaneously. This finding is robust across all three primary user activity regimes evaluated, confirming that the operating point is a property of the framework architecture rather than an artefact of specific channel loading. From a deployment perspective, ten interchangeable edge nodes represent the practical coordination target for general-purpose SpaaS operation, while configurations exceeding this density remain appropriate for ultra-reliable or mission-critical slices where maximum interference protection is required regardless of overhead cost.

Three directions are identified for future investigation. First, experimental validation on USRP-based software-defined radio platforms integrated with live CBRS or LSA spectrum management infrastructure would provide empirical grounding for the simulation gains reported here and quantify the practical impact of multipath fading, synchronization imperfections, and control-plane latency on the ISSS performance envelope, enabling direct comparison with deployed SAS-based architectures. Second, extending the framework to ad-hoc non-stationary spectrum environments through online or reinforcement learning would allow the sensing cost and detection quality parameters to adapt as channel occupancy statistics evolve beyond the stationary birth–death model assumed in this work, improving ISSS responsiveness under dynamic real-world conditions. Third, evaluating ISSS across licensed and unlicensed spectrum bands by relaxing the primary user priority constraint — effectively removing priority constraint from the joint allocation objective of Section 3.5 — would quantify how governance-free operation affects the interference reduction, spectrum utilization, and scheduling efficiency gains reported here, providing a comparative performance baseline for deployment contexts where incumbent protection is not a binding regulatory requirement. Together, these directions map a path toward a fully autonomous, regulation-aware, and environmentally adaptive spectrum orchestration layer capable of operating across the governance boundaries and physical-layer conditions of beyond-5G and 6G wireless networks.

Author Contributions: Conceptualization, S.S., I.E. and I.M.; methodology, S.S. and I.E.; software, I.E. and A.A.; validation, I.E., I.M. and A.A.; formal analysis, S.S., I.E. and I.M.; investigation, S.S. and I.E.; writing—original draft preparation, S.S.; writing—review and editing, S.S., I.E., I.M., A.A. and A.A.E.; visualization, A.A. and I.E.; supervision, A.A.E. and I.M.; project administration, S.S. All authors have read and agreed to the published version of the manuscript.

Funding: This research received no external funding.

 doi:10.20944/preprints202605.0218.v1

Data Availability Statement: The pseudocode, system model, simulation parameters, and numerical results supporting the findings of this study are fully described within the manuscript. Readers wishing to access the complete simulation implementation may contact the corresponding author upon reasonable request.

Acknowledgments: During the preparation of this manuscript, the authors used ChatGPT (OpenAI, GPT-4, web interface, https://www.chatgpt.com) and Claude (Anthropic, Claude Sonnet, web interface, https://www.claude.ai) for the purposes of formatting, layout, and general readability of the text, and to support the verification of simulation code by converting the original MATLAB implementation to Python for cross-validation of the reported results. These tools were not used to generate scientific content, derive analytical results, or draw conclusions. The authors have reviewed and edited the output and take full responsibility for the content of this publication.

Conflicts of Interest: The authors declare no conflicts of interest.:

Abbreviations

The following abbreviations are used in this manuscript:

ISSS	Interchangeable Spectrum Sensing Scheduling
SpaaS	Spectrum-as-a-Service
5G	Fifth Generation
6G	Sixth Generation
MEC	Multi-Access Edge Computing
CBRS	Citizens Broadband Radio Service
LSA	Licensed Shared Access
PU	Primary User
SLA	Service-Level Agreement
URLLC	Ultra-Reliable Low-Latency Communication
IoT	Internet of Things
RAN	Radio Access Network
CR	Cognitive Radio

References

1. Popovski, P.; Trillingsgaard, K.F.; Simeone, O.; Durisi, G. 5G wireless network slicing for eMBB, URLLC, and mMTC: A communication theoretic view. IEEE Access 2018, 6, 55765–55779. https://doi.org/10.1109/ACCESS.2018.2872781
2. Abouaomar, A.; Cherkaoui, S.; Mlika, Z.; Kobbane, A. Resource provisioning in edge computing for latency-sensitive applications. IEEE Internet Things J. 2021, 8, 11088–11099. https://doi.org/10.1109/JIOT.2021.3052082
3. Patil, A.; Prasad, R.; Skouby, K.E.; Prasad, N.R. A comprehensive survey on spectrum sharing techniques for 5G/B5G intelligent wireless networks. Comput. Netw. 2024, 224, 109608. https://doi.org/10.1016/j.comnet.2023.109608
4. Bhattarai, S.; Park, J.M.; Gao, B.; Bian, K.; Lehr, W. A survey on Citizens Broadband Radio Service. Electronics 2022, 11, 3891. https://doi.org/10.3390/electronics11233891
5. Massaro, M.; Beltrán, F. Untangling the paradox of Licensed Shared Access: Need for regulatory refocus. Telecommun. Policy 2022, 46, 102380. https://doi.org/10.1016/j.telpol.2022.102380
6. Akyildiz, I.F.; Lo, B.F.; Balakrishnan, R. Cooperative spectrum sensing in cognitive radio networks: A survey. Phys. Commun. 2011, 4, 40–62. https://doi.org/10.1016/j.phycom.2010.12.003
7. Ghasemi, A.; Sousa, E.S. Spectrum sensing in cognitive radio networks: Requirements, challenges and design trade-offs. IEEE Commun. Mag. 2008, 46, 32–39. https://doi.org/10.1109/MCOM.2008.4481338

 doi:10.20944/preprints202605.0218.v1

8. Federal Communications Commission (FCC). Report and Order and Second Further Notice of Proposed Rulemaking, FCC 15-47; FCC: Washington, DC, USA, 2015. Available online: https://www.fcc.gov/document/fcc-15-47 (accessed on 1 May 2025).
9. Ofcom. TV White Spaces: Consultation on White Space Device Requirements; Ofcom: London, UK, 2012. Available online: https://www.ofcom.org.uk/spectrum/spectrum-management/tv-white-spaces (accessed on 1 May 2025).
10. Kryszkiewicz, P.; Kliks, A.; Kułacz, Ł.; Bogucka, H.; Koudouridis, G.P.; Dryjański, M. Context-based spectrum sharing in 5G wireless networks based on radio environment maps. Wirel. Commun. Mob. Comput. 2018, 2018, 3217315. https://doi.org/10.1155/2018/3217315
11. ETSI. MEC Support for Edge Native Design: An Application Developer Perspective; White Paper No. 55; ETSI: Sophia Antipolis, France, 2023. Available online: https://www.etsi.org/deliver/etsi_wp/55_99/55/01.01.01_60/wp_055e.pdf (accessed on 1 May 2025).
12. Taleb, T.; Samdanis, K.; Mada, B.; Flinck, H.; Dutta, S.; Sabella, D. On multi-access edge computing: A survey of the emerging 5G network edge cloud architecture and orchestration. IEEE Commun. Surv. Tutor. 2017, 19, 1657–1681. https://doi.org/10.1109/COMST.2017.2705720
13. Moubayed, A.; Ahmed, T.; Haque, A.; Shami, A. Machine learning towards enabling Spectrum-as-a-Service dynamic sharing. In Proceedings of the IEEE Canadian Conference on Electrical and Computer Engineering (CCECE), London, ON, Canada, 30 August–2 September 2020. https://doi.org/10.1109/CCECE47787.2020.9255741
14. ITU-R. SM.2405-1: Spectrum Management Principles for Cognitive Radio Systems; ITU: Geneva, Switzerland, 2021. Available online: https://www.itu.int/rec/R-REC-SM.2405/en (accessed on 1 May 2025).
15. Salih, S.H.O.; Erman, M.; Mohammed, A. A novel spectrum sensing scheduling algorithm for cognitive radio networks. In Self-Organization and Green Applications in Cognitive Radio Networks; IGI Global: Hershey, PA, USA, 2012; pp. 136–153. https://doi.org/10.4018/978-1-4666-0050-8.ch006
16. Latif, S.; Akraam, S.; Karamat, T.; Khan, M.A.; Altrjman, C.; Mey, S.; Nam, Y. An efficient Pareto-optimal resource allocation scheme in cognitive radio-based Internet of Things networks. Sensors 2022, 22, 451. https://doi.org/10.3390/s22020451
17. Mitola, J.; Maguire, G.Q. Cognitive radio: Making software radios more personal. IEEE Pers. Commun. 1999, 6, 13–18. https://doi.org/10.1109/98.788210
18. Haykin, S. Cognitive radio: Brain-empowered wireless communications. IEEE J. Sel. Areas Commun. 2005, 23, 201–220. https://doi.org/10.1109/JSAC.2004.839380
19. IEEE Standard for Policy Language for Dynamic Spectrum Access Systems. IEEE Std. 1900.5.1-2020; IEEE: Piscataway, NJ, USA, 2020. https://doi.org/10.1109/IEEESTD.2020.9120108
20. 3GPP. Service Requirements for the 5G System; Technical Specification TS 22.261, Release 18; 3rd Generation Partnership Project: Sophia Antipolis, France, 2024. Available online: https://www.3gpp.org/specifications-technologies/releases/release-18 (accessed on 2 May 2026).
21. ITU-R. Framework and Overall Objectives of the Future Development of IMT for 2030 and Beyond; Recommendation ITU-R M.2160-0; International Telecommunication Union: Geneva, Switzerland, 2023. Available online: https://www.itu.int/rec/R-REC-M.2160/en (accessed on 2 May 2026).
22. Hossain, E.; Vera-Rivera, A. 6G cellular networks: Mapping the landscape for the IMT-2030 framework. IEEE Commun. Surv. Tutor. 2025, online first. https://doi.org/10.1109/COMST.2025.3560786.
23. Robert, C.P.; Casella, G. Monte Carlo Statistical Methods, 2nd ed.; Springer: New York, NY, USA, 2004; ISBN 978-0-387-21239-5.